INTENSE THERMAL ELECTRON-ION BEAM PROPAGATION PROPERTIES WITH NO APPLIED MAGNETIC FIELD*

C. D. Striffler, R. L. Yao, and X. Zhang

Electrical Engineering Department
and
Laboratory for Plasma and Fusion Energy Studies
University of Maryland, College Park, MD 20742

Summary

A steady-state, electron-ion beam propagation model is presented that self-consistently determines the downstream equilibrium properties of co-moving electron and ion beams in terms of upstream properties. Since there is no applied magnetic field, the presence of the ions is crucial to the downstream equilibrium. The ions are assumed to come from a localized source located near the entrance end of the injected electron beam. Each species has finite temperature in addition to a mean axial velocity. Downstream radial force balance leads to a Bennett radial density profile. Continuity of current and conservation of single particle energy lead to the self-consistent nature of the equilibrium and the determination of the localized ion source properties to achieve the equilibrium. The main quantitative result from the model is that an electron temperature exists where the equilibrium is nearly charge neutral and the ion mean velocity is near zero, that is, the ions provide no current neutralization. If the ion temperature is zero, this state represents the "traditional" Bennett pinch system.

Introduction

The propagation of intense relativistic electron beams is important to such diverse fields as high power coherent radiation development, collective ion acceleration, and plasma heating and confinement. The field of intense beams and some of their uses are presented in a book by R. B. Miller.[1] The specific system studied in this paper involves an intense electron beam injected into an evacuated cylindrical drift tube through a localized source of ions. The ions are required in order to have beam propagation since no applied magnetic field is present. Experimental results[2,3] indicate that under "optimized" conditions effective beam propagation occurs to distances of 50 cm.

A schematic of our system is shown in Fig. 1. An electron beam is injected with voltage V_o and current I_o into a long drift tube of radius R_w. In order to have electron beam propagation, ions are provided by a region immediately downstream of the injection surface. The properties of this localized source region are its formation rate S_i (C/sec) and potential V_{io} at which the ions are created. Of course, a charge neutralizing electron species is simultaneously formed. The ions and electrons are then able to propagate downstream with the ions initially at rest gaining kinetic energy as they fall through the potential difference $V_{io} - V$, and the beam electrons losing kinetic energy due to the downstream potential depression V. This localized region can be formed by electron beam ionization of a neutral gas cloud[4] or preformed by laser irradiation of a target. The combination of the injected electron beam and localized source is able to create the large localized space charge fields for the ions to gain the needed energy for beam propagation downstream. The downstream

electron-ion beam is assumed to have a mean axial electron velocity $V_{ze} = \beta_{ze}c$ and a mean axial ion velocity $V_{zi} = \beta_{zi}c$. Each species has a temperature, T_e and T_i, and we assume that, in general, there is no charge neutrality and/or current neutrality, thus resulting in a self-electric field E_{sr} and self-magnetic field $B_{s\phi}$. The goal of this paper is to interrelate all the system parameters. In the next section, a Vlasov particle distribution for each species is presented. The macroscopic quantities are derived and then radial force balance, along with continuity of current and conservation of single particle energy, is applied. Initial results from this model have been presented.[2,5,6]
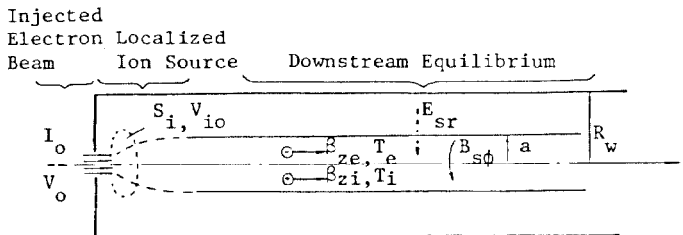
FIG. 1. Schematic of the model.

Vlasov Distribution

The starting point for our model is the assumption that the particle distribution function for each component of the downstream beam is a relativistic Maxwellian in the frame traveling at the fluid velocity of the component.[7] In particular, we assume that in the frame traveling with the fluid velocity $\beta_{zj}c$, the distribution function for that component is

$$f_j(\underset{\sim}{x},\underset{\sim}{p}) = a_j \exp[-\frac{(p^2c^2 + m_j^2c^4)^{1/2} + q_j V^{(j)}}{kT_j^{(j)}}] , \quad (1)$$

where a_j is a normalization constant chosen so that $\int d^3p f_j$ equals the local particle density, $V^{(j)}$ is the potential in that frame, and $T_j^{(j)}$ is the temperature of the component in that frame.

Macroscopic Equations and Conservation Constraints

From the above particle distributions, we can show that the downstream radial force balance equation becomes in the laboratory frame

$$q_j n_j(r)[E_{sr}(r) - V_{zj}B_{s\phi}(r)] - kT_j \frac{dn_j(r)}{dr} = 0 , \quad (2)$$

where the self-fields are given by

$$E_{sr}(r) = \frac{e}{\epsilon_o r} \int_0^r [Zn_i(r') - n_e(r')]r'dr' \quad (3)$$

and

$$B_{s\phi}(r) = \frac{\mu_o e}{r} \int_0^r [Zn_i(r')V_{zi} - n_e(r')V_{ze}]r'dr' , \quad (4)$$

and T_e and T_i are the species temperature in the laboratory frame. The solution to the above equations is (with $Z = 1$)

$$n_e(r) = \frac{n_{eo}}{[1 + (r/a)^2]^2} = \frac{n_{eo}}{n_{io}} n_i(r) , \qquad (5)$$

where

$$n_{eo} = \frac{8\epsilon_o}{e^2 a^2} \frac{kT_e(1 - \beta_{zi}^2) + kT_i(1 - \beta_{ze}\beta_{zi})}{(\beta_{ze} - \beta_{zi})^2} \qquad (6a)$$

$$n_{io} = \frac{8\epsilon_o}{e^2 a^2} \frac{kT_e(1 - \beta_{ze}\beta_{zi}) + kT_i(1 - \beta_{ze}^2)}{(\beta_{ze} - \beta_{zi})^2} \qquad (6b)$$

which are the familiar Bennett pinch density profiles. We note that unlike previous derivations of the Bennett pinch equilibrium,[8-10] our derivation does not assume that the axial velocity of the particles is much greater than the transverse velocities. We note that in general the electrons are confined by the self-magnetic field and the ions by the self-electric field. The effective radius of each species is "a." These solutions in the limit $T_i = 0$ have been presented.[11]

We now apply to the downstream equilibrium two system constraints. Continuity of current for each species gives, for electrons

$$I_{ot} = \frac{8\pi\epsilon_o c\beta_{ze}}{(\beta_{ze} - \beta_{zi})^2} \left[\frac{kT_e}{e} (1 - \beta_{zi}^2) + \frac{kT_i}{e} (1 - \beta_{ze}\beta_{zi})\right]$$

$$\times \frac{(R_w/a)^2}{1 + (R_w/a)^2} , \qquad (7)$$

where I_{ot} is the transmitted electron beam current, and for ions

$$S_i = \frac{8\pi\epsilon_o c\beta_{zi}}{(\beta_{ze} - \beta_{zi})^2} \left[\frac{T_e}{e} (1 - \beta_{ze}\beta_{zi}) + \frac{kT_i}{e} (1 - \beta_{ze}^2)\right]$$

$$\times \frac{(R_w/a)^2}{1 + (R_w/a)^2} . \qquad (8)$$

Conservation of single particle energy gives, for electrons

$$1 + \frac{eV_o}{m_e c^2} + \frac{eV(0)}{m_e c^2} = \overline{\gamma}_e \frac{K_3(\alpha_e)}{K_2(\alpha_e)} - \frac{kT_e}{m_e c^2} , \qquad (9)$$

for ions

$$1 + \frac{eV_{io}}{m_i c^2} - \frac{eV(0)}{m_i c^2} = \overline{\gamma}_i \frac{K_3(\alpha_i)}{K_2(\alpha_i)} - \frac{kT_i}{m_i c^2} , \qquad (10)$$

where $\overline{\gamma}_j = (1 - \beta_{zj}^2)^{-1/2}$, $\alpha_j = m_j c^2/\overline{\gamma}_j kT_j$, $j = \{e,i\}$, $V(0)$ is the downstream potential evaluated on-axis, and K_3 and K_2 are modified Bessel functions.

The solution procedure for the above set of equations is as follows. We assume that I_{ot}, V_o, R_w/a, T_e, and T_i are known and then solve for β_{ze}, β_{zi}, S_i, V_{io}. In addition, we can compute the net current

$$I_{net} = \frac{8\pi\epsilon_o c}{\beta_{zi} - \beta_{ze}} (\frac{kT_e}{e} + \frac{kT_i}{e}) \frac{(R_w/a)^2}{1 + (R_w/a)^2} , \qquad (11)$$

and the fractional charge neutralization

$$f = \frac{n_i}{n_e} = \frac{(1 - \beta_{ze}^2)T_i + (1 - \beta_{ze}\beta_{zi})T_e}{(1 - \beta_{ze}\beta_{zi})T_i + (1 - \beta_{ze}^2)T_e} . \qquad (12)$$

These quantities are plotted in the next section.

Graphical Results and Discussion

A set of typical results from our model is presented in Fig. 2. Specifically, we have $V_o = 1$ MV, $R_w/a = 10$, and $T_i = 0$ and have plotted β_{ze}, β_{zi}, V_{io}, S_i and I_{net}, $V(0)$, and f versus T_e with I_{ot} as a parameter. One of the main features of these results is that a temperature T^* exists where $\beta_{zi} = 0$. For example, if $I_{ot} = 5$ kA, $T_e^* \simeq 60$ keV, and if $I_{ot} = 30$ kA, $T_e^* \simeq 250$ keV. Acceptable equilibria exist on for $T_e < T_e^*$, since the region above T_e^* requires the localized source to be far downstream from the injected electron beam. We note that at T_e^*, the system is charge neutral, $V(0) = 0$ and $f = 1.0$, and the net current is due only to the electrons, $I_{net} = I_{ot}$. This point is the traditional Bennett state. We find that temperatures just below this value provide system parameters that are very close to the calculated avalanche conditions of a localized gas cloud. This temperature T^* is less than 250 keV for currents up to 25 kA and a diode voltage of 1 MV. This temperature is reasonable for beam systems that have injected currents high enough so that virtual cathodes form. If we fix the electron current I_{ot} and vary the electron voltage V_o, we find that the temperature T_e^* decreases.

In Fig. 3, we display the effects of finite ion temperature. We have plotted I_{net} and f versus T_e with T_i as a parameter. The other fixed system parameters are $V_o = 1$ MV, $I_{ot} = 20$ kA, and $R_w/a = 10$. The effects of finite ion temperature are to lower the value of the critical temperature T_e^* and in turn eliminate the existence of a charge neutral state. That is, the state of no current neutralization (zero ion velocity) still occurs at T_e^*, but this state requires a net negative charge.

We have found self-consistent downstream equilibria between electrons and ions with no applied axial magnetic field. The electrons are confined by the self-magnetic field and the ions by the self-electric field. In addition, the model calculates the required localized ion source properties necessary to achieve the equilibrium. The system is self-consistently derived from a relativistic Maxwellian particle distribution for each species.

References

1. R. B. Miller, An Introduction to the Physics of Intense Charged Particle Beams, Plenum, New York, 1982.
2. W. W. Destler, et al., Beams '86, Sixth Int. Conf. on High Power Particle Beams, June 9-12, 1986, Kobe, Japan.
3. W. W. Destler, et al., accepted for publication in J. Appl. Phys., April 1987.
4. H. Dantsker, et al., Bull. APS 29, 1353 (1984).
5. Z. Segalov, et al., Bull. APS 30, 1505 (1985).
6. X. Zhang, et al., Bull. APS 31, 1429 (1986).
7. R. L. Yao, submitted to Phys. of Fluids, March 1987.
8. W. H. Bennett, Phys. Rev. 45, 890 (1934).
9. E. P. Lee, Phys. Fluids 19, 60 (1976).
10. R. C. Davidson, et al., Phys. Fluids 22, 1375 (1979).
11. R. J. Faehl, et al., IEEE Trans. Nucl. Sci. NS-32, 3500 (1985).
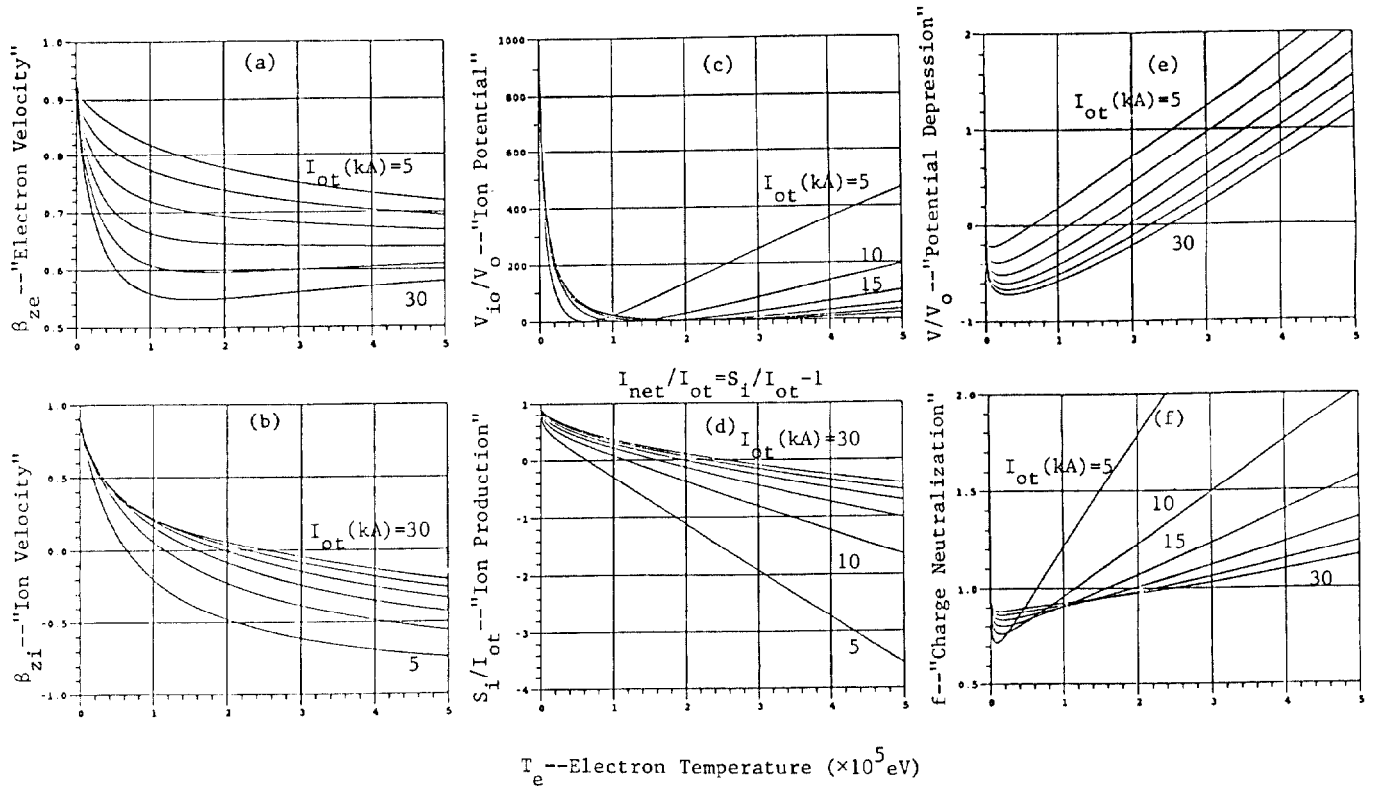
FIG. 2. Normalized electron velocity, ion velocity, ion potential, ion production rate and net current, potential depression, and fractional charge neutralization versus electron temperature with electron current a parameter. Fixed parameters; $V_o = 1$ MV, $R_w/a = 10$, and $T_i = 0$.
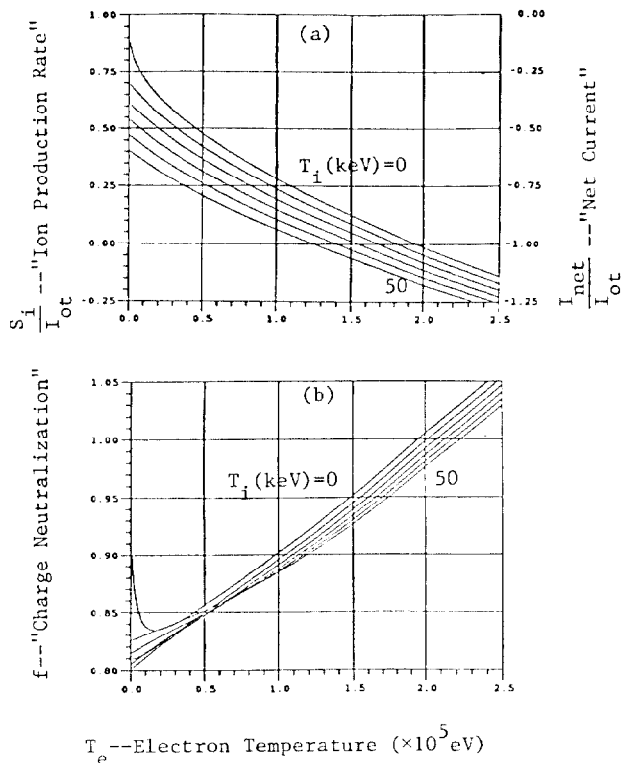
FIG. 3. Normalized net current (a) and fractional charge neutralization (b) versus electron temperature with ion temperature a parameter. Fixed parameters; $V_o = 1$ MV, $I_{ot} = 20$ kA, and $R_w/a = 10$.